

MOLECULAR CYTOLOGY AND CYTOMETRY

HEAD

STANISLAV KOZUBEK

GROUP OF STRUCTURE AND FUNCTION OF THE CELL NUCLEUS

GROUP LEADER

EVA BÁRTOVÁ

SCIENTISTS

GABRIELA GALIOVÁ, LENKA STIXOVÁ

PHD. STUDENTS

SOŇA LEGARTOVÁ, DARYA ORLOVA

DIPLOMA STUDENTS

RADKA UHLÍŘOVÁ, ALŽBĚTA JUGOVÁ

TECHNICAL ASSISTANT

JANA KŮROVÁ

BC STUDENT

PETRA SEHNALOVÁ

HP1 protein and epigenetics of nucleoli

We utilized immunofluorescence combined with high-resolution Nipkow disc-based confocal microscopy to visualize the localization of some epigenetic factors in control and SUV39h deficient cells. In addition, the cells were treated with TSA, an inhibitor of histone deacetylases (HDACi). HP1 subtypes were shown to localize at the periphery of the nucleoli, associating with the clusters of pericentromeric heterochromatin called chromocenters. Thus, we determined how SUV39h deficiency and HDACi influenced the presence of HP1 and H3K9 di- and tri-methylation at the chromocenters. This was then compared to similar epigenetic marks within nucleoli. Analyses of HP1 subtypes confirmed different interphase patterns in SUV39h (wt) and SUV39h (dn) cells (Fig. 1 and 2a-d). For example, in the control cells, HP1 alpha was strictly associated with chromocenters, while HP1 beta was observed not only in the chromocenters, but also in the chromatin-poor regions in close proximity to the chromocenters (Harničarová-Horáková et al., 2009). HP1 gamma associated equally with chromocenters and the surrounding chromatin in SUV39h (wt) cells. As expected, SUV39h deficiency and HDACi in wild type cells significantly reduced the levels of all HP1 subtypes at the chromocenters (Harničarová-Horáková et al., 2009).

Following elucidation of HP1 nuclear pattern, we examined the presence of all HP1 subtypes inside the nucleoli, which consist of fibrillar centers (FC), dense fibrillar components (DFC), and granular components (GC). Fibrillarin (ribose 2'-O-methylase), which specifically interacts with small nucleolar RNAs (snoRNAs), is located in DFC. In both SUV39h (wt) and SUV39h (dn) cells, the HP1 alpha and HP1 gamma subtypes were associated with fibrillarin-positive regions to smaller extent, when compared with HP1 beta that strictly co-localized with fibrillarin (Fig. 1). This nucleolus-associated location was observed for HP1 beta, not only in the mouse model studied, but also to a lesser extent in human small lung carcinoma A549 cells and mouse fibroblasts lacking the LMNA gene that encodes A-type lamins (published by Harničarová-Horáková et al., Chromosoma 2009). The association of fibrillarin-positive regions with HP1 beta was also confirmed in SUV39h (wt) and SUV39h (dn) cells transiently expressing GFP-HP1 beta (Fig. 1). Indeed, we observed a high density of GFP-HP1 beta protein in fibrillarin-positive regions of the nucleoli. In addition to the influence of Suv39h deficiency on the epigenetics and structure of nucleoli, we studied whether HDACi can influence the presence of select epigenetic markers inside the nucleoli. Both the absence of SUV39h and HDACi decreased H3K9me2 inside the nucleoli, and these changes were more pronounced after TSA treatment of SUV39h (dn) cells. On the other hand, we observed that in the fibrillarin-positive region, H3K9me3 and HP1 beta levels were relatively stable compared to the chromocenters of identical cells. This implies that both Suv39h deficiency and HDAC inhibition have a subtle impact on some epigenetic profiles and epigenetic stability of DFC where fibrillarin is located.

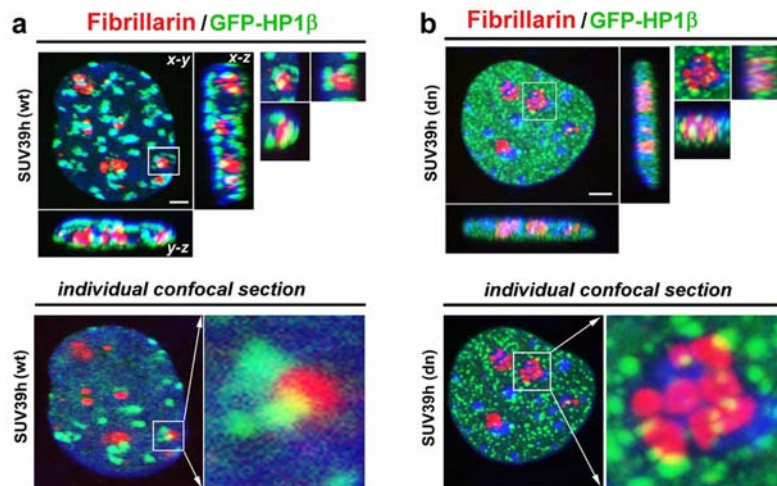


Figure 1: SUV39h (wt) and SUV39h (dn) cells expressing GFP-HP1 beta and fibrillarin localization. a) SUV39h (wt) b) SUV39h (dn) fibroblasts transiently expressing GFP-HP1 beta (green), subsequently stained by antibody against fibrillarin (red). In both the cases tested, fibrillarin co-localized with HP1 beta foci. Scale bars represent 1 micrometer.

Optimization of FRAP technique and DNA repair studies

We have study dynamic properties of chromatin-related proteins, including HP1 subtypes (Fig. 2), histone demethylase JMJD2b, beta-catenin, BMI1, TRF1 or c-MYC in Suv39h (wt), (dn) fibroblasts and in LMNA deficient cells. In selected experimental systems, we analyzed dynamics of chromatin-related proteins and we would like to find the factors that are responsible for kinetics properties of individual proteins. FARP technique was sufficiently optimized in our laboratory; therefore, we would like to continue with such experiments.

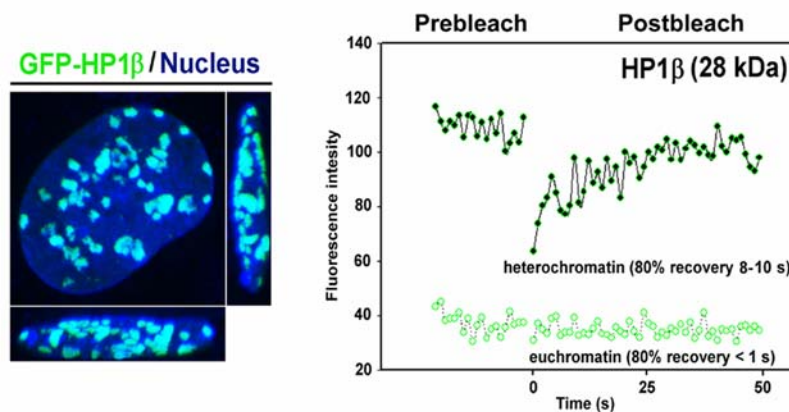


Figure 2: Example of HP1 β kinetics in euchromatin and heterochromatin in (wt) mouse fibroblasts. As observed by other authors (Cheutin et al., 2003), there is distinct kinetics between HP1 β accumulated in euchromatin and HP1 β that binds to heterochromatin regions. By the use of GFP-HP1 β plasmid we were able to optimize FRAP technique in our laboratory.

In other experiments, double strand breaks (DSBs) were induced by 355 nm UV laser and, following local DNA damage, the presence of phosphorylated H2.AX (gamma H2A.X) was detected as a marker of DSBs (Fig. 3). U2OS cells stably expressing GFP-BMI1 were cultivated under standard conditions and in these cells we analyzed recruitment of Polycomb group (PcG)-related protein BMI1 to DSBs. At 70% confluence, the cells were sensitized with 10 microM BrdU, 16-18 h before local irradiation. Cells were irradiated by UV laser (355 nm). We irradiated half of the nuclei or strips of nuclei by 80% laser output, not reduced at AOTF. The

following settings were used: 512×512 pixels, 400 Hz, bidirectional mode, 64 lines, zoom >5-10. Irradiated cells were fixed in 4% paraformaldehyde and phosphorylated histone H2A.X (gamma H2AX) was detected with rabbit polyclonal antibody to gammaH2A.X (phospho S139) (Abcam, #ab2893) in immunofluorescence and confocal microscopy.

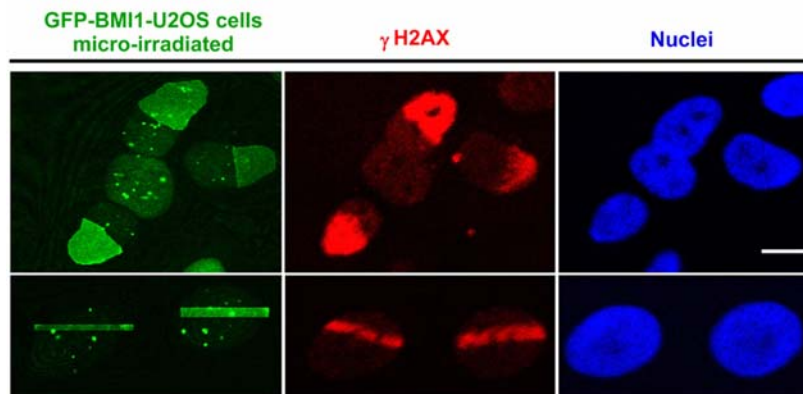


Figure 3: Relationship of BMI1 protein to DSBs induced by micro-irradiation was tested. (A) GFP-BMI1-U2OS (green) cells were micro-irradiated by UV laser (355 nm) and the induction of DSBs was verified using antibody against gammaH2AX (red areas or strips). Bar represents 20 μ m. Cells were counterstained by Hoechst 33342.

GROUP OF THE STRUCTURE, FUNCTION AND DYNAMICS OF CHROMATIN

GROUP LEADER

EMILIE LUKÁŠOVÁ

SCIENTIST

MARTIN FALK

SPECIALIST

ALENA BAČÍKOVÁ

Higher-order chromatin structure in DSB induction, repair and misrepair

Cell survival and maintenance of genome integrity are dependent on the efficient and accurate repair of DNA double-strand breaks (DSBs) mediated by exogenous agents but also during execution of DNA function. Cellular response to DNA DSBs consists of complex signaling network that coordinates initial recognition of the lesion with the induction of its repair. However the access of enzymes and regulatory factors to the sites of DSBs is hampered by highly complicated three-dimensional structure of chromatin especially in its condensed regions. The loosening of chromatin in the vicinity of DSBs is necessary to recruit and maintain activities of repair proteins. Our results show that this chromatin loosening results in local changes in chromatin structure and can influence the probability of mutual interaction of DSBs. DSBs repair takes place, in principle, at the sites of their induction; however, as a consequence of chromatin decondensation, some DSBs protrude into a sparse chromatin (chromatin holes) where they could potentially cluster and form complex lesions that are repaired only with difficulties and pose an increased risk of chromosomal translocation formation. According to the proposed model (Falk et al., 2010), the DSB repair may significantly change the probabilities of DSB interactions derived from nuclear distances of the damaged loci, in the dependence of local higher-order chromatin structure (Fig. 4).

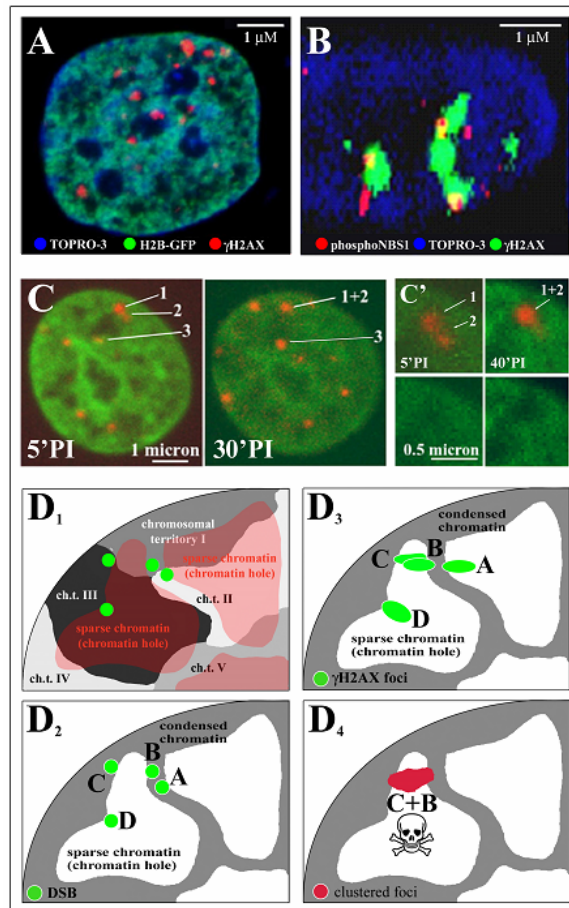


Figure 4: A model showing the relationships between higher-order chromatin structure, DSB repair and formation of chromosomal translocations. (A) x–y central slice through a spatially fixed MCF7 cell nucleus shows the location of γ H2AX foci (red), induced with 1.5 Gy of γ -rays, relative to dense and sparse chromatin domains, 10 min PI. Chromatin density is reflected by the intensity of H2B-GFP (green) and TOPRO-3 (blue) staining. Dark areas represent nucleoli and “chromatin holes”. (B) Clustering of γ H2AX foci shown in 3D space (x-z plane) in spatially fixed normal human fibroblasts irradiated with 3 Gy of γ -rays. γ H2AX foci (green) observed 2 h PI; NBS1 (red), chromatin (TOPRO-3, blue). (C) Central slices (0.4 μ m x–y plane) of human MCF7 cells double-transfected with 53BP1-RFP and H2B-GFP proteins, irradiated with a dose of 1.5 Gy of γ -rays, displayed at 5 min and 30 min PI, show re-localization of 53BP1 foci 2 and 3 (red) from dense to sparse chromatin. After this relocalization, focus 2 formed a cluster with focus 1; this cluster persisted until the end of observation (40 min PI, enlarged detail at panel C0). Chromatin density, green (H2B-GFP). (D) Proposed model of the relationship between higher-order chromatin structure, DSB repair and formation of chromosomal translocations. (D1) Schematic location of chromosomal territories that could be subject to chromatin exchange during DSB repair. (D2) The higher-order chromatin structure and Brownian movement of chromatin determine the original radius of mutual DSB (γ H2AX foci, green) interactions. Heterochromatin between A and B prevents their mutual interaction. (D3) chromatin decondensation at sites of DSBs induced at the boundary of eu- and heterochromatin can significantly increase (foci B and C) or decrease (foci A and B) the original probability of interactions between DSBs. (D4) Foci B and C are at the highest risk of chromatin exchanges despite the shortest nuclear distance being between foci A and B. (Figure is adopted from Falk et al.,2010).

Molecular mechanisms of the cell death in leukemia cells caused by DNA damage during exposure of cells to fractionated irradiation in vitro

We studied the effect of fractionated irradiation with γ -rays on ability of human cells of lymphocytic leukemia MOLT4 to repair DNA DSBs. Our results show that many cells are not able to accomplish repair of all induced DNA DSBs before application of the next radiation dose. The long presence of unrepaired DSBs induced by the fractionated irradiation represents long-term genotoxic stress leading to elimination of cells with this damage. Process elimination of cells containing non repaired DSBs after irradiation depends on the mode of radiation dose delivery. In single irradiation with the high radiation dose inducing high number of DNA DSBs, the prevailing process of cell elimination is apoptosis. During fractionated irradiation with lower doses, three different processes participate on elimination of cells with unrepaired DSBs - apoptosis, genotoxic-stress-induced cellular senescence and adaptation to active checkpoint G2 when the cells enter the mitoses and majority of them die during this process. Our results are the first showing induction of massive cellular senescence and active checkpoint adaptation of leukemia cells exposed to long-term DNA damage during fractionated irradiation used for radiotherapy of tumors.

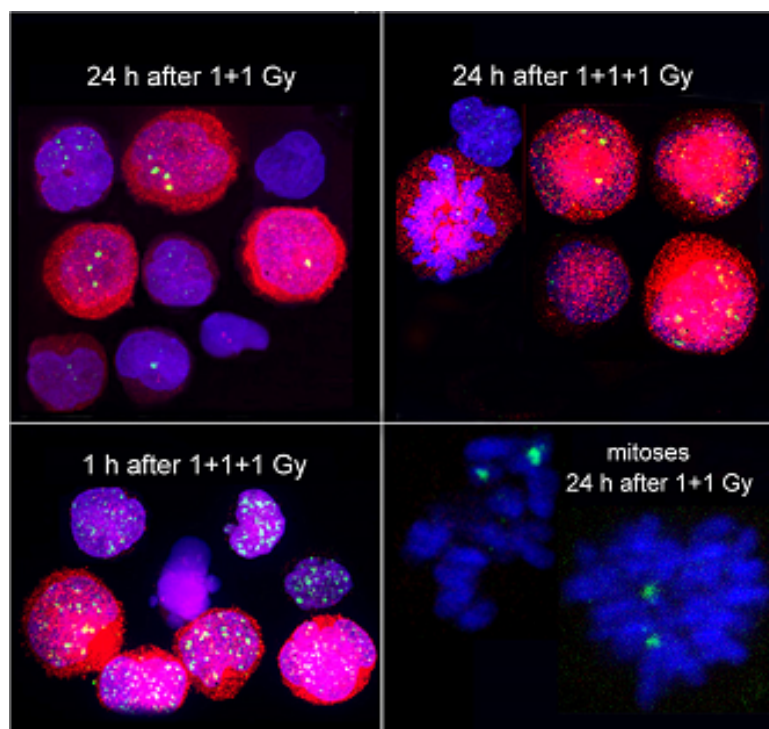


Figure 5: Cyclin B1 expression in Molt 4 cells arrested in G2 phase during repeated irradiation with the doses of 1 Gy in the interval of 24 h indicates that the cells are entering the mitosis in spite of unrepaired DSBs in their DNA. Representative projection of Molt 4 cells expressing high level of cyclin B1 (red) at the time 24 h after the doses of 2 x 1 Gy; 1 and 24 h after 3 x 1 Gy. Non repaired DSBs (green) are seen also at some chromosomes (blue) during mitosis. After the single doses of 1 Gy and 3 Gy, as well as after the cumulative dose 4 x 1 Gy, cells with high level of cyclin B1 were observed neither 24 nor 48 h PI. 1h after IR with the third dose, the cells contained high number of DSBs, represented by green foci of γ -H2AX, however 23 h later, the number of these foci decreased indicating that cells repaired DNA damages in spite of their presence at the boundary of mitoses. The cells with high level of cyclin B1 (red) were determined after immunodetection by counting on microscopic slides in visual field of confocal microscope among 500 cells per sample.

GROUP OF THE ANALYSIS OF CHROMOSOMAL PROTEINS

HEAD OF THE RESEARCH GROUP

MICHAL ŠTROS

SENIOR SCIENTISTS

JIRÍ FAJKUS, EVA ŠYKOROVÁ, MILOSLAVA FOJTOVÁ, JANA FULNEČKOVÁ

PHD. STUDENTS

EVA POLANSKÁ, ZUZANA KUNICKÁ, MARTINA DVOŘÁČKOVÁ, VRATISLAV PEŠKA, LUCIA GULÁŠOVÁ

TECHNICAL ASSISTANT

LIBUŠE JEDLIČKOVÁ, KATEŘINA ŠIPKOVÁ

DNA topoisomerase II α and HMGB proteins: a search for a common link

We have continued in our recently published studies dealing with the effect of HMGB1/2 proteins on the activity and cellular expression of human topoisomerase II α (Štros et al: Nucleic Acids Res. 2007, 2009). Our results pointed out a correlation between over-expression of topoisomerase II α and HMGB1/2 in human cancer cell lines. Our results also provided evidence that mechanism of HMGB1-mediated stimulation of activity of topoisomerase II α was due to enhanced DNA cleavage which was further promoted by topo II poisons. Higher cellular expression (and activity) of topoisomerase II α by HMGB1/2 proteins in Rb-minus cells, as well as the stimulatory effect of HMGB1 on activity of topoisomerase II α , could have clinical relevance in respect to

prognosis of patients treated with topoisomerase II poisons. This idea is supported by the fact that HMGB1/2 proteins are frequently reported to be over-expressed in cancer, and Rb deletions are observed in most tumors (the project is also conducted in collaboration with Š. Pospíšilová from Center of Molecular Biology and Gene Therapy, University Hospital Brno).

Modulation of telomerase activity by HMGB1 in mouse and human cells

Eukaryotic chromosome stability relies on the presence of intact chromosome ends or telomeres. Telomeres are formed by a special chromatin structure that protects chromosome termini from recombination and degradation, thus preventing end-to-end chromosome fusions and other chromosomal aberrations. Telomeres are replicated by telomerase. Here we have demonstrated that HMGB1 could interact *in vitro* with telomerase catalytic component TERT and RNA component TR. However, once telomerase is formed, the interaction of HMGB1 with telomerase seems to be weak or undetectable. In support, only a weak telomerase activity could be detected upon immunoprecipitation of cellular lysates with α -HMGB1 antibody. As reconstitution of telomerase has previously been reported *in vitro* with only TERT and TR (rabbit reticulocyte lysate), we have initiated experiments aiming at understanding of a possible modulatory effect of HMGB1 on telomerase assembly *in vitro*. We have also demonstrated a stimulatory effect of recombinant HMGB1 on the activity of telomerase in cellular lysates, explaining our previous findings revealing decreased activity of telomerase in HMGB1 knocked out mouse embryonic fibroblasts or human MCF-7 cells with inhibited HMGB1 expression.

Single-Myb-histone proteins from *Arabidopsis thaliana*: a quantitative study of telomere-binding specificity and kinetics

Proteins that bind telomeric DNA modulate the structure of chromosome ends and control telomere function and maintenance. It has been shown that AtTRB (*Arabidopsis thaliana* telomere repeat-binding factor) proteins from the SMH (single-Mybhistone) family selectively bind double-stranded telomeric DNA and interact with the telomeric protein AtPOT1b (*A. thaliana* protection of telomeres 1b), which is involved in telomere capping. In the present study, we performed the first quantitative DNA-binding study of this plant-specific family of proteins. Interactions of full-length proteins AtTRB1 and AtTRB3 with telomeric DNA were analysed by electrophoretic mobility-shift assay, fluorescence anisotropy and surface plasmon resonance to reveal their binding stoichiometry and kinetics. Kinetic analyses at different salt conditions enabled us to estimate the electrostatic component of binding and explain different affinities of the two proteins to telomeric DNA. On the basis of available data, a putative model explaining the binding stoichiometry and the protein arrangement on telomeric DNA has been generated.

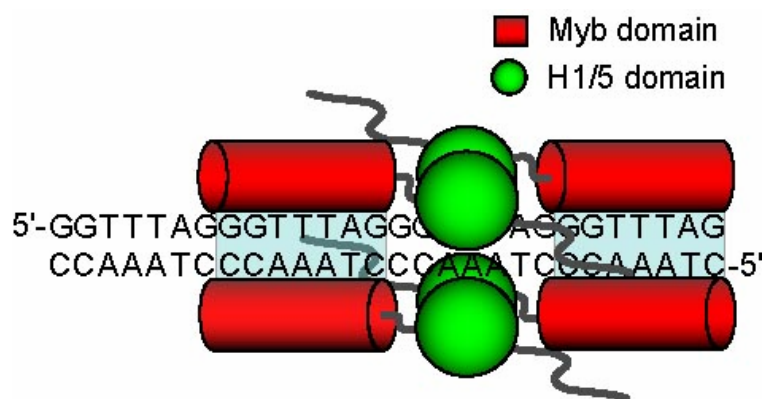


Figure 6: Speculative model of interaction of AtTRBs with telomeric DNA Both homo- and hetero-dimers of AtTRB may participate in the interaction with telomeric DNA. (Hofr et al., *Biochem. J.* 2009)

AtTRB1, a telomeric DNA-binding protein from *Arabidopsis*, is concentrated in the nucleolus and shows highly dynamic association with chromatin. AtTRB1, 2 and 3 are members of the SMH (single Myb histone) protein family, which comprises double stranded DNA-binding proteins that are specific to higher plants. They are structurally conserved, containing a Myb domain at the N-terminus, a central H1/H5-like domain and a C-terminally located coiled-coil domain. AtTRB1, 2 and 3 interact through their Myb domain specifically with telomeric double-stranded DNA *in vitro*, while the central H1/H5-like domain interacts non-specifically with DNA sequences and mediates protein-protein interactions. We showed that AtTRB1, 2 and 3 preferentially localize to the nucleus and nucleolus during interphase. Both the central H1/H5-like domain and the Myb domain from AtTRB1 can direct a GFP fusion protein to the nucleus and nucleolus. AtTRB1-GFP localization is

cell cycle-regulated, as the level of nuclear-associated GFP diminishes during mitotic entry and GFP progressively re-associates with chromatin during anaphase/telophase. Using fluorescence recovery after photobleaching and fluorescence loss in photobleaching, we determined the dynamics of AtTRB1 interactions in vivo. The results reveal that AtTRB1 interaction with chromatin is regulated at two levels at least, one of which is coupled with cell-cycle progression, with the other involving rapid exchange.

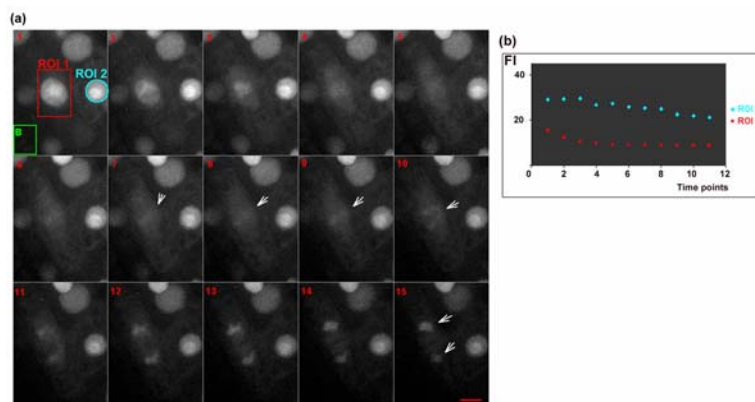


Figure 7. AtTRB1 dynamics during mitosis. (a) Time-lapse images of *A. thaliana* C24 plants expressing GFP-AtTRB1 followed during the cell cycle at 1 min intervals. GFP-AtTRB1 is re-localized from the nucleolus and nucleus at the beginning of mitosis (1–3); a detectable level of GFP-AtTRB1 associated with mitotic chromatin persists (arrowed in 7–10) and re-integrates into newly formed nucleoli (arrowed in 15). Background fluorescence intensity was measured in the boxed area marked B. Scale bar = 5 μm. (b) Estimation of fluctuation in GFP-AtTRB1 fluorescence intensity in the mitotic region (ROI 1, red line) and the control region (ROI 2, blue line) in scans 1-11. The fluorescence intensity in the mitotic region (ROI 1, red line) decreases rapidly at the beginning of mitosis, and it becomes stabilized over the following stages. Overall sample bleaching is approximately 30% (blue line). Fluorescence intensity measurements were performed using IMAGEJ software (Dvořáčková et al., Plant J. 2010).

GROUP OF EXPERIMENTAL HEMATOLOGY

GROUP LEADER

MICHAL HOFER

SENIOR SCIENTISTS

MILAN POSPÍŠIL, ANTONÍN VACEK, ZUZANA HOFEROVÁ, LENKA WEITEROVÁ

RESEARCH FELLOW

JIŘINA HOLÁ

TECHNICAL ASSISTANT

KVĚTA LÁNÍKOVÁ

In 2009, we made further progress in our studies aimed at evaluation of the hematopoiesis-modulating effects of adenosine receptor agonists and cyclooxygenase-2 inhibitors, as well as at understanding their mechanisms. An inhibitor of cyclooxygenase-2, meloxicam, has been shown to increase the production of erythropoietin (EPO) (Table 1) and to elevate numbers of hematopoietic progenitor cells committed to erythroid cell lineage (burst-forming units, BFU-E) in mice irradiated with a sublethal dose of 4 Gy of gamma-rays. This is an interesting finding because previous findings concerned predominantly stimulatory effects of cyclooxygenase inhibitors on granulopoiesis. The results may have impact also in clinical practice if cyclooxygenase-2 inhibitors will be used for treatment of myelosuppression of various etiology.

Unirradiated control mice		
48.3 ± 18.1		
Irradiated mice		
Time interval after injection (hours)	Saline-treated controls	Meloxicam-treated mice
6	206.0 ± 86.6*	433.1 ± 87.6#
12	186.3 ± 16.1*	421.4 ± 82.6#

Table 1: Serum concentrations of EPO (pg/ml) in 4 Gy-irradiated mice after administration of meloxicam in a single dose on day 3 after irradiation.

Mice were administered saline or meloxicam in a single dose on day 3 after irradiation. Serum concentration of EPO was determined 6 and 12 hours after the injection. Data are given as means \pm S.E.M. Five animals per group were used. * - $P < 0.05$ vs. unirradiated control mice; # - $P < 0.05$ vs. irradiated saline-treated mice.

An adenosine A3 receptor agonist, IB-MECA, was tested for its ability to induce the growth of colonies growing from hematopoietic progenitor cells for granulocytes and macrophages (GM-CFC) in suspension of normal mouse bone marrow cells in vitro and to potentiate stimulatory effects of hematopoietic growth factors (interleukin-3 /IL-3/, stem cell factor /SCF/, granulocyte-macrophage colony-stimulating factor /GM-CSF/, and granulocyte colony-stimulating factor /G-CSF/) on these cells. Whereas IB-MECA alone induced no GM-CFC colony growth, a significant increase in GM-CFC numbers has been observed when IB-MECA was added to the cultures concomitantly with IL-3, SCF, or GM-CSF. These findings give evidence of a significant role played by selective activation of adenosine A3 receptors in the regulation of the growth of granulocyte/macrophage hematopoietic progenitor cells.